# **RESEARCH ARTICLE**

# PLC $\gamma$ has a dual role in capsaicin-triggered neurogenic inflammation promoting mechanical hypersensitivity and edema in male mice

© Alexandre M. do Nascimento,<sup>1,2</sup> © Ana M. Rodrigues,<sup>1</sup> © Heloisa E. G. Ramos,<sup>1</sup> © Beatriz C. de Moraes,<sup>1</sup> © Raphael S. Santos,<sup>1</sup> © Camila S. Dale,<sup>2</sup> and © Deborah Schechtman<sup>1</sup>

<sup>1</sup>Department of Biochemistry, Chemistry Institute, University of São Paulo, São Paulo, Brazil and <sup>2</sup>Laboratory of Neuromodulation of Experimental Pain (LaNed), Department of Anatomy, Institute of Biomedical Sciences, University of São Paulo, São Paulo, Brazil

#### **Abstract**

Understanding the signaling mechanisms leading to neurogenic inflammation, a process found in chronic pain, psoriasis and migraine, is key for the development of more effective analgesics. A key player in the onset of this inflammation is transient receptor potential cation channel, subfamily V, member 1 (TRPV1), an ion channel abundant at the free terminals of nociceptors, which can be directly activated by capsaicin (CAP), acidic pH or noxious heat, and indirectly through phospholipase C-γ (PLCγ), which promotes cleavage of the inhibitory phosphatidylinositol-4,5-bisphosphate from the channel. In turn, PLCγ is activated via its phosphorylation by growth factor receptor tyrosine kinases, such as the high affinity nerve growth factor receptor, tropomyosin kinase A (TrkA). We previously developed a permeable phosphopeptide (TAT-pQYP) that binds to PLCγ, preventing lipase anchoring to TrkA, and hence its phosphorylation/activation, and showed that PLC $\gamma$  is key for mechanical hypersensitivity in CFA-induced inflammation. Herewith, we investigate the role of PLC $\gamma$  in an acute model of inflammatory nociception induced by the subcutaneous injection of CAP in the hind paw of male mice. This model elicited a two phase response, the first related to TRPV1's sensitization and the latter to neurogenic inflammation. TAT-pQYP did not alter the TRPV1-mediated chemonociceptive response and neurogenic signaling itself, but it was able to disrupt PLCγ signaling, reverting nerve growth factor/TrkA-dependent mechanical hypersensitivity in nociceptors, and returning paw diameter to baseline levels by disrupting vascular endothelial growth factor A/endothelial nitric oxide synthase signaling in endothelial cells. Altogether, our results show that TAT-pQYP disrupts PLCy signaling in CAP-triggered neurogenic inflammation, leading to an anti-inflammatory and antinociceptive effect without interfering with TRPV1 chemosensitivity and neuropeptides activity. PLC represents a potential target to relieve neurogenic inflammation-dependent pain while preserving TRPV1's physiological activity.

**NEW & NOTEWORTHY** When activated, TRPV1 promotes neurogenic inflammation via neuropeptide signaling. However, drugs designed to directly block TRPV1 may impair its nociceptive roles, essential for tissue preservation. In this work, pain and swelling caused by neurogenic inflammation were mitigated after blocking PLC $\gamma$ 's activity, modulating TRPV1's activity without affecting normal chemosensitivity. This suggests that blocking PLC $\gamma$  could be a new approach for the development of painkillers maintaining the physiological detection of harmful stimuli.

analgesia; inflammatory pain; nociception; pain mechanisms; phospholipase Cγ

## INTRODUCTION

Pain is an emotional and sensorial aversive experience typically caused by lesion or potential tissue damage. Nociceptive pain is perceived by normal functioning nociceptors (1). Nociceptors can be sensitized through their membrane channels, including transient receptor potential cation channel, subfamily V, member 1 (TRPV1), which can be activated by noxious heat, acidic environments, and vanilloids (2, 3). Binding of the exovanilloid ligand capsaicin (CAP) to TRPV1 enhances expression and release of proinflammatory neuropeptides, substance P (SP) and calcitonin gene-related peptide (CGRP), in peptidergic nociceptors, leading to the recruitment

of immune cells that mediate the inflammatory process (4). Among them, the recruitment and degranulation of mast cells triggered by SP is important for the release of multiple proinflammatory molecules, including nerve growth factor (NGF) (5). In turn, NGF activates its high affinity receptor tyrosine kinase (RTK), tropomyosin kinase A (TrkA), substantially expressed in nociceptors, thereby creating a neuro-immune inflammatory feedback loop (6). Upon NGF-TrkA interaction, multiple signaling pathways are activated (7), including activation of phospholipase  $C-\gamma$  (PLC $\gamma$ ) (8, 9), which hydrolyses phosphatidylinositol-4,5-bisphosphate (PIP2) to diacylglycerol (DAG) and inositol 1,4,5-trisphosphate (IP3), promoting calcium efflux from the endoplasmic reticulum mediated by





IP3 receptors and influx via TRPV1 opening by releasing the channel from PIP2 inhibition (8, 10). Calcium and DAG are also essential for activation of protein kinase C (PKC), which can phosphorylate TRPV1, sustaining channel activity (11).

Many compounds were designed to directly modulate pain signaling in nociceptors by directly inhibiting NGF, TrkA, or TRPV1. Several of these have been tested in clinical trials and shown to be very effective in mitigating pain (12). However, side effects due to downstream inhibition of other important signaling pathways, such as Akt and ERK, which are involved in neurite outgrowth and neuronal survival in the case of NGF/TrkA (13), and inhibition of normal thermal and chemical nociceptive activity of TRPV1 (14), have been reported. Thus, elucidating signaling pathways that are more specific to the inflammatory pain processes is key for the development of more effective analgesics that do not compromise physiological activity of their targets (13, 15).

In this context, our group previously designed a permeable phosphopeptide (TAT-pQYP) based on mutations identified in patients with congenital insensitivity to pain with anhidrosis (CIPA) that could lead to a truncated TrkA, lacking the PLCγ's binding site, necessary for the phosphorylation/activation of the lipase (16). Likewise, TAT-pQYP prevents PLCy's anchoring to TrkA by binding to the lipase's SH2 domain, disrupting its activation (17). Intraplantar injection of TAT-pQYP attenuated complete Freund's adjuvant (CFA)induced mechanical hypersensitivity, in a similar fashion to Trk and PLC inhibitors (17), underscoring the role of PLC $\gamma$  signaling in inflammatory pain mediated by NGF in nociceptors.

Here, we used subcutaneous injection of CAP in the hind paws of mice, to evaluate how PLC<sub>γ</sub> is implicated in TRPV1dependent inflammatory nociceptive pain phenotypes. Using TAT-pQYP as a tool to disrupt PLC $\gamma$  signaling by inhibiting its interaction with RTKs, we show the interplay between TrkA, PLCγ, and TRPV1 in chemosensitivity and mechanical hypersensitivity. Furthermore, we show that RTK signaling via PLC $\gamma$  is also relevant in endothelial cells by contributing to the increase in paw diameter during neurogenic inflammation. Taken together, we suggest that targeting PLCγ in pain mechanisms that rely on neurogenic inflammation could lead to more effective pain management strategies.

#### MATERIALS AND METHODS

## **Cell Culture and Western Blot**

Neuro2A cells (mouse neuroblastoma cells, ATCC No. CCL-131) were maintained in high-glucose Gibco Dulbecco's modified Eagle medium (DMEM) supplemented with NaHCO<sub>3</sub> (3.7 g/L), 1 mM sodium pyruvate, penicillin (100 U/mL), streptomycin (100 μL/mL), and 10% fetal bovine serum, at 37°C and 5% CO<sub>2</sub>. Cells were cultured in six wells plates until they reached 80% confluency, when they were transiently transfected in Opti-MEM (Gibco by Life Technologies) using polyethylenimine (3 µg/well) and 1 µg/well of Ntrk1 (TrkA) DNA (obtained from G. Lewin, Max Delbruck Center for Molecular Medicine, in an eucaryotic expression plasmid with resistance gene for ampicillin; pEXPR IBA 105). Six hours after transfection medium was replaced by complete culture medium, and cells were cultured for another 48 h.

Cells were then starved for 12 h in serum-free culture medium and incubated with either, TAT, TAT-QYP, or TAT-

pQYP (0.8 μM) for 30 min and treated with 100 ng/mL β-recombinant human NGF (Cat. No. 450-01, PeproTech) for 5 min. Concentrations of peptides and NGF were determined based on previous studies. Cells were then lysed in 70 µL of lysis buffer [1% Triton X-100, 20 mM TRIS, pH 7.4, 100 mM NaCl, 1× protease (SIGMAFAST, Sigma-Aldrich), and 2× phosphatase (PhosSTOP, Roche) inhibitors]. Lysates were sonicated (30 pulses) and centrifuged at 16,000 RCF for 15 min at 4°C. The supernatant was collected and fully mixed in a 1:4 ratio with 5× Laemmli buffer (0.125 M Tris-HCl, pH 6.8, 4% SDS, 20% glycerol, 10% 2-mercaptoethanol, and 0.004% bromophenol blue) and heated to 95°C for 5 min. Lysates were then run on 7.5% SDS-PAGE, which were subsequently transferred to 7.5% polyacrylamide gel was loaded with proteins for electrophoresis, before proteins were transferred to a PVDF membranes in a wet-transfer system (Bio-Rad). Membranes were dried for at least 1 h before blocking with LI-COR Intercept Blocking Buffer. Blotts were probed with primary antibodies against total TrkA (Cat. No. A4147, AbClonal, 1:1,000), total PLCγ (Cat. No. 2822, Cell Signaling, 1:1,000), phospho-PLCγ Tyr<sup>783</sup> (Cat. No. 2821, Cell Signaling, 1:100), phospho-MARCKS Ser $^{152/156}$  (Cat. No. 2741, Cell Signaling, 1:500),  $\alpha$ -tubulin (Cat. No. A11126, Thermo Fisher Scientific, 1:3,000) diluted in blocking buffer (SuperBlock Blocking Buffer, Thermo Fisher Scientific) containing 0.1% tween-20 and incubated overnight at 4°C. Membranes were washed five times for 5 min in T-TBS (20 mM Tris-base, 150 mM NaCl, 0.1% Tween-20, pH 7.6) and incubated for 2 h with IRDve 800CW donkey anti-rabbit (1:15,000) or IRDye 680CW donkey anti-mouse (1:15,000) at room temperature, protected from light. Images were acquired using LI-COR Odyssey DLx imaging system, and densitometry of the immunoreactive bands were carried out using ImageJ software.

## **Animals**

Isogenic male C57BL/6NTac mice from 8 to 10 wk old (20–26 g) were used for behavioral assessment and tissue extraction. Animals were housed at the following conditions: 21 ± 2°C room temperature, tap water ad libitum, and NuVital ration, 4 or 5 mice/house cage, 12/12 dark/light cycle. Mice were acclimated to the animal facility for 1 wk before any behavioral test. Animals were randomly assigned to groups, with blinding of the experimenter, who performed all behavioral analysis and in vivo measurements. Sample size was calculated using 80% statistical power and 95% confidence interval. All animal protocols were previously approved by the competent ethics committee of the Institute of Biomedical Sciences of the university of São Paulo (CEUA 4121050423) and designed according to ARRIVE 2.0 guidelines (18).

#### **Drugs and Substances**

All drugs or substances were injected subcutaneously (sc) to the dorsal surface of the hind paw using 29 G needles in a 20 uL volume. Baseline (BSL) behavioral assessments were performed at least 30 min before the first injection. Inhibitors were diluted in 1% DMSO: Capsazepine (CPZ; Sigma Aldrich, Cat. No. C191; 100 pmol/paw) (19); U-73122 (Sigma Aldrich, Cat. No. 662035; 100 pmol/paw); GNF-5837 (Sigma Aldrich, Cat. No. SML0844; 2 μmol/paw) (17). Proalgesic substances and peptides were diluted and used in the following

concentrations: β-recombinant human NGF (Cat. No. 450-01, PeproTech), 500 ng/paw in distilled water (20); CAP (Cat. No. 0462, Tocris), 2.00 µg/paw in 10% ethanol and 10% tween-20 (19); peptides (obtained from Chinese Peptide), 1.6 µmol/paw in distilled water (17). Peptides sequences are linked (GSG linker) to human immunodeficiency virus-1 TAT peptide (GRKKRRQRRRPQ) for intracellular delivery (21) and the respective sequences are: TAT-pQYP (GRKKRRQRRRPQGSGQAPPVpYLDVLG), TAT-QYP (GRKKRRQRRRPQGSGQAPPSYLDVLG), and pQYP (QAPPSpYLDVLG) (17). All experiments were conducted in a vehicle-paired fashion, using 1% DMSO when involving CPZ, U-73122, and GNF-5837, distilled water for NGF or peptides only, and 10% ethanol/10% tween-20 solution as a control for CAP.

#### **Behavioral Assays**

Capsaicin test (CAP test) was performed on an acrylic apparatus in front of a mirror for better visualization. Mice were injected with CAP and immediately placed in the apparatus for filming. Time spent licking and biting the injected hind paw was assessed for 5 min and the results expressed as nociceptive response to CAP (s) (19).

Von Frey test was performed to determine mechanical sensitivity according to up-down method (22). In brief, nylon monofilaments (North Coast Medical) 0.07 g, 0.16 g, 0.4 g, 0.6 g, 1.0 g, 1.4 g, 2.0 g, 4.0 g, and 6.0 g were used to build a sensitivity profile of the plantar region of the hind paw, interpreted by:  $0.5 g = 10 [Xf + k\gamma]$ , where Xf is the logarithmic of the last monofilament applied, k is the constant value correspondent to the sequence of six responses (positive: withdrawal; negative: no response), and  $\gamma$  is the logarithmic mean of the monofilaments used. Results are expressed as 50% paw withdrawal threshold (g).

For mechanical sensitivity to innocuous touch, the 0.07 g monofilament was applied six consecutive times to the hind paw, in intervals of at least 30 s. For mechanical sensitivity to noxious touch, a 24 G needle was applied 10 times to the hind paw with no skin perforation, in intervals of at least 3 min (23). Mice that exhibited a maximum response to the stimulations at the BSL test were excluded from data analysis.

#### **Paw Diameter Assessment**

The diameter of the hind paw was assessed using a digital caliper. Mice were kept in their housing cages during the experiments and had their paws measured at the same site, determined at the BSL measure, during the experimental time course.

#### RT-qPCR

Mice were euthanized by 2% isoflurane inhaling and had their death confirmed by cervical dislocation. Paws were collected and stored immediately on dry ice. RNA extraction was performed using the TRIzol kit (Thermo Fisher), and cDNA was obtained using the SuperScript IV kit (Thermo Fisher), according to manufacturer instructions. RT-qPCR was run according to standard amplification protocols using SYBR green fluorescent probe (Thermo Fisher). Quantitation was performed by the  $2^{-\Delta\Delta Ct}$  method, using Gapdh as a housekeeping control (24). Primers used for the different genes were: Ngf forward 5'-GGGAGCGCATTCGAGTGAC-3'; Ngf reverse 5'-CAAAACTCCACCATGCTGCC-3'; Vegfa forward 5'-CCCAGAGAGCAGGTGGTTTA-3'; Vegfa reverse 5'-TGCCCTTCTCCTTCTG-3'; Gapdh forward 5'-ACTTCA-ACAGCAACTCCCACT-3'; Gapdh reverse 5'-TGGGTGGTCC-AGGGTTTCTTA-3'.

#### **Immunofluorescence**

L4-L6 ipsilateral DRGs (dorsal root ganglia) were collected and fixed embedded in 4% paraformaldehyde (in 0.1 M phosphate buffer) for 24 h before moving to a 30% sucrose solution (in 0.1 M phosphate buffer) for long term storage. Tissues were processed in optimal cutting temperature at  $-35^{\circ}$ C, and 12 μm sections were obtained using a cryostat on SuperFrost Plus slides, which were latter blocked in 10% normal goat serum and 0.05% Tween-20, in phosphate buffered saline, followed by incubation in 0.3 M glycine with 0.2% Tween-20 for 20 min. Primary antibody against CGRP (Cat. No. 14959, Cell Signaling) was diluted 1:300 in the blocking buffer and incubated at 4°C overnight. After washing 2 times each for 10 min in PBS, sections were incubated with secondary antibody (Cat. No. A-21428, goat anti-rabbit Alexa Fluor 555, Thermo Fisher, 1:1,000) for 2 h at 4°C, and washed two times for 10 min in PBS. Glass slides were mounted with Fluoromount-G (Thermo Fisher Scientific). Images were captured using ZEISS Axio Observer, and two image fields from each animal, and a total of three animals per group, were analyzed with ImageJ.

#### **Western Blot of Tissue**

Ipsilateral paws were dissected and automatically homogenized in RIPA buffer (25 mM Tris-HCl pH 7.6, 150 mM NaCl, 1% IGEPAL, 1% sodium deoxycholate, 0.1% SDS, EDTA 5 mM) with 10% protease (SIGMAFAST, Sigma-Aldrich) and phosphatase (PhosStop, Roche) inhibitors. Lysates were centrifuged at 16,000 RCF for 20 min at 4°C, and the supernatant was collected. Total protein content was quantified using bicinchoninic acid (BCA) assay quantification kit (Thermo Fisher Scientific). Protein (40 µg) were prepared for SDS-PAGE in Laemmli buffer and heated to 70°C for 10 min. SDS-PAGE and transfer of gels to PVDF membranes was performed as described in Cell Culture and Western Blot section. Blotts were probed with total eNOS (Cat. No. 9586, Cell Signaling, 1:1,000), phospho-eNOS Ser<sup>1177</sup> (Cat. No. 9570, Cell Signaling, 1:1,000). Membranes were then reprobedfor total eNOS after stripping using NewBlot LI-COR PVDF stripping buffer, incubated with IRDye 800CW donkey anti-rabbit (1:15,000) and developed as described in Cell Culture and Western Blot section.

#### Histochemistry

Glabrous skin from injected paws were collected and fixed in 4% paraformaldehyde (in 0.1 M phosphate buffer) for 24 h before moving to a 30% sucrose solution (in 0.1 M phosphate buffer) for long term storage. Tissues were mounted in paraffin and 16 µm longitudinal sections were obtained. Sections were stained with toluidine blue to assess mast cells distribution in the tissue (25). Tissues were processed by the São Paulo University Institute of Biomedical Sciences histotechnology facility, and micrographs were obtained using brightfield high-resolution objectives. Sections from three mice for each group were assessed. Three image fields from individual mice were analyzed, and the results were averaged for multiple comparison analysis. Cell counts were performed by an experimenter blinded to treatments using Image-Pro Plus (version 6.0). Background cells are blue-stained after toluidine blue, whereas mast cells could be identified as violet metachromatic structures. Among them, spread granules and cloudy surroundings were counted as degranulating mast cells.

## **Statistical Analysis**

Normality of samples was assessed by fitting data to a normal distribution. Unpaired t test was used to assess differences between two groups. One-way or two-way ANOVA tests were used for three or more groups, when appropriate, with Tukey post hoc test for significance assessment (P value < 0.05). All statistical analysis and graphs were generated using the software GraphPad PRISM (10.3 version).

## RESULTS

## TAT-pQYP Inhibits PLCy and Downstream PKC-**Mediated Signaling**

We started assessing TAT-pQYP's capacity to inhibit PLCγ activation and downstream signaling in Neuro2A cells transiently expressing TrkA after NGF stimulus. We observed that TAT-pQYP, but not TAT carrier alone or the peptide lacking the phosphorylated Tyr (TAT-QYP), decreased PLC<sub>Y</sub>

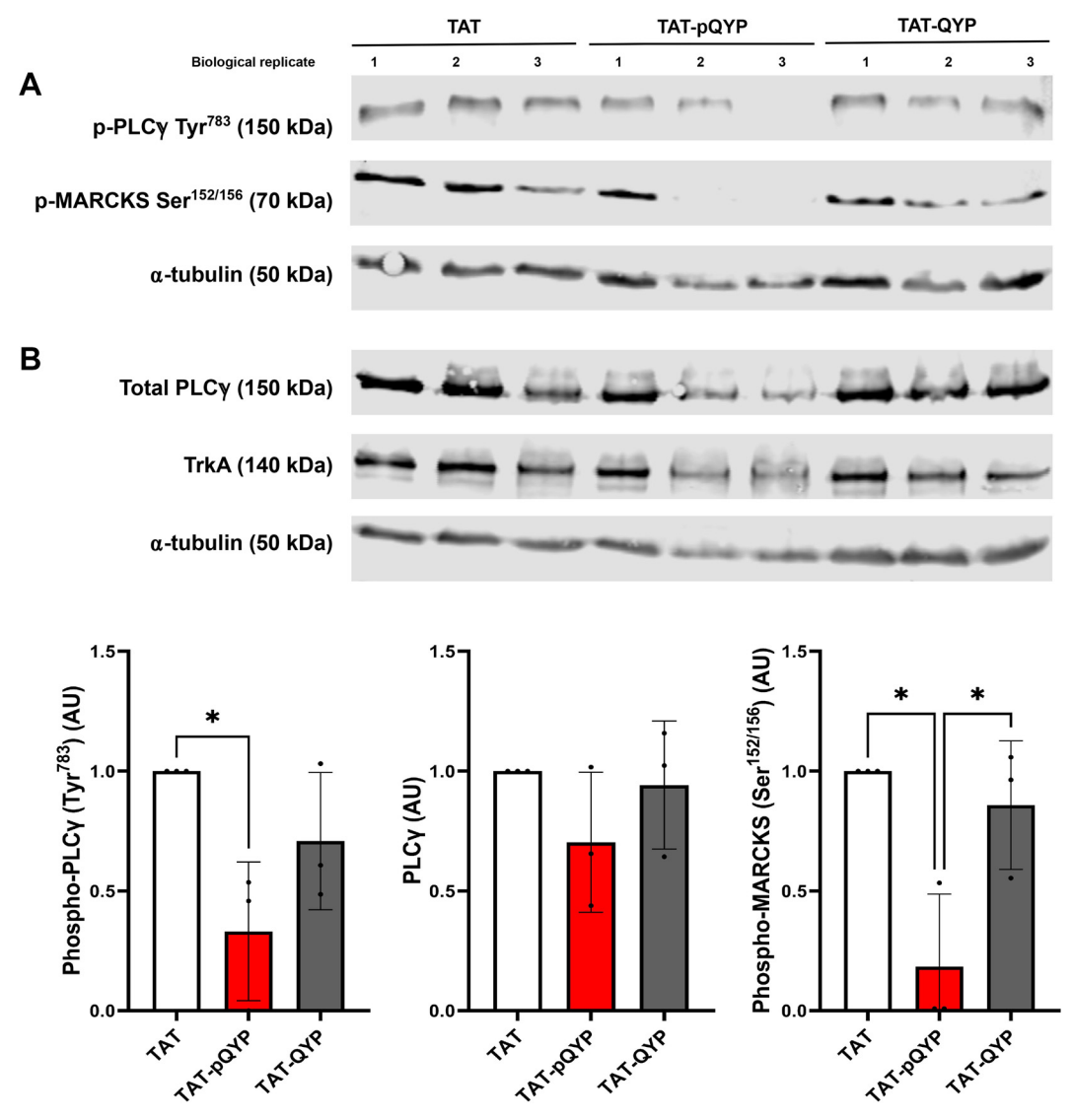
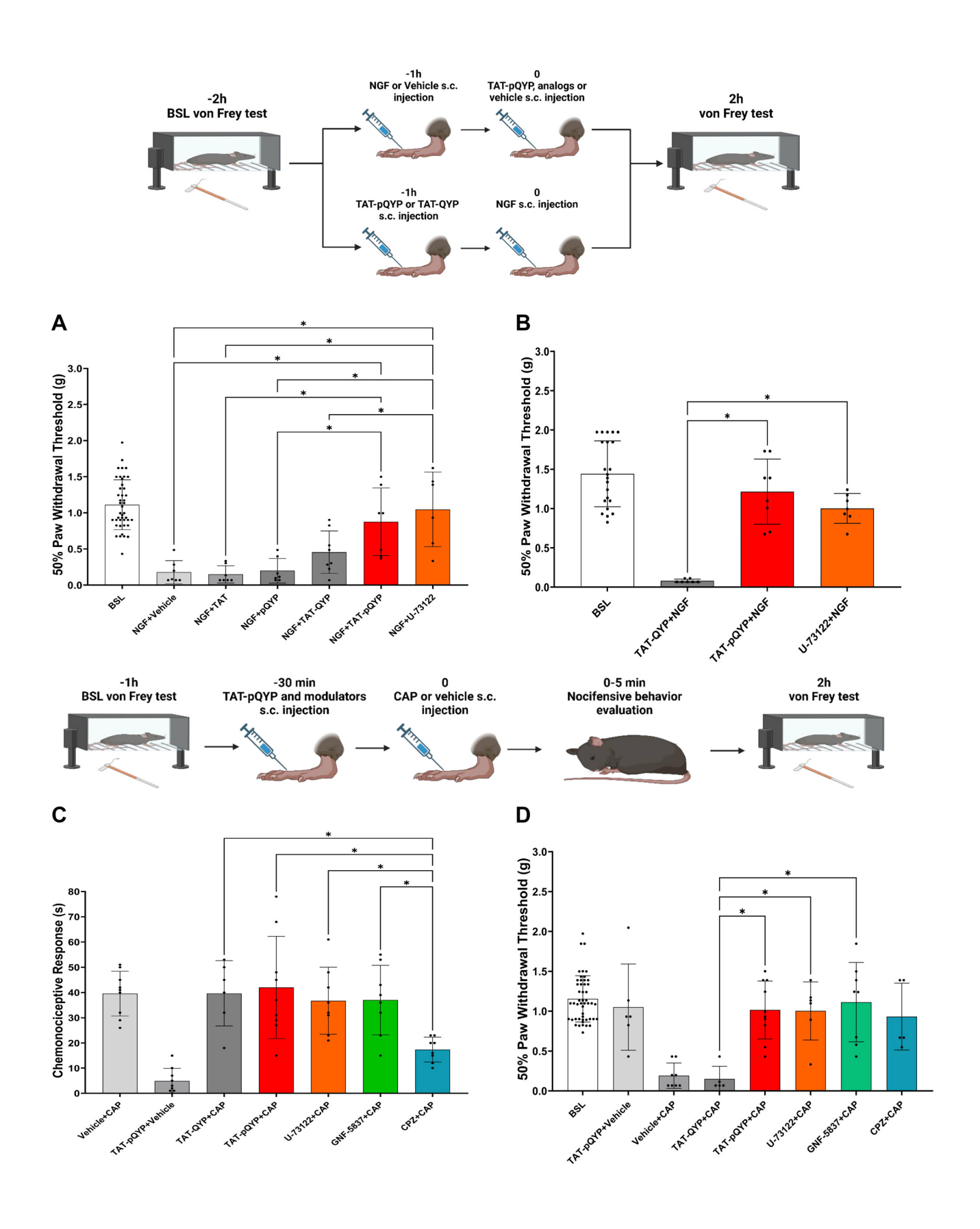


**Figure 1.** TAT-pQYP prevents TrkA mediated PLC $\gamma$  and PKC activation in NGF-treated transfected Neuro2A cells. *A, top*: Western blot showing that TAT-pQYP, but not TAT or TAT-QYP, decreased both PLC $\gamma$  and MARCKS phosphorylation as seen with anti-p-PLC $\gamma$  (Tyr<sup>783</sup> residue) and anti-p-MARCKS (Ser<sup>152/156</sup> residue). Blots were probed with anti α-tubulin for normalization. B: Western blot of a separate gel with the same lysates probed for total PLCγ, total TrkA, and  $\alpha$ -tubulin. Each gel contains three independent experiments (N = 3). Bottom: quantitative representation of gels (A and B), where independent experiments are presented as black dots, and average ± SD is indicated. Densitometric values of the immunoreactive bands panel (A and B) were normalized to α-tubulin, and individual experiments were compared with their respective control group (density of the TAT group), which was considered the maximal activation for each biological replicate. Multiple comparison analysis was performed by one-way ANOVA followed by Tukey's post hoc test to determine statistical significance. \*P < 0.05. NGF, nerve growth factor; PKC, protein kinase C; PLC $\gamma$ , phospholipase C- $\gamma$ ; TrkA, tropomyosin kinase A.





phosphorylation at Tyr<sup>783</sup> (Fig. 1A), a phosphorylation necessary for lipase activation (17), whereas PLC<sub>γ</sub> expression levels are not different between groups (Fig. 1B), these effects were similar to the previously observed with HEK-293T cells expressing TrkA (17). To assess the effect on PLC $\gamma$ -mediated downstream signaling, blots were probed for a protein kinase C (PKC) substrate, phosphorylated myristoylated alaninerich C kinase substrate (MARCKS) (26). Since, PKC activation requires PLC activity/generation of DAG (11). As expected, TAT-pQYP was able to decrease MARCKS phosphorylation at Ser<sup>152/156</sup> (Fig. 1A), supporting the fact that TAT-pQYP inhibits PLC<sub>Y</sub> and PKC signaling, further supporting pathway disruption by the peptide.

## PLC<sub>γ</sub> Activity Does Not Modulate the Immediate TRPV1-Related Chemonociceptive Response to CAP, but it Participates in the Later TrkA-Mediated Mechanical Hypersensitivity

We next tested whether injection of 1.6 μmol/paw of TATpQYP, previously associated with PLCy inhibition and a decrease in mechanical hypersensitivity mediated by CFA (17), would promote an antinociceptive effect upon exogenous NGF injection. Using pan-PLC inhibitor U-73122 (27) as a positive control, we found that only full length TAT-pQYP, but not peptide lacking the phosphorylated Tyr (TAT-QYP) neither the intracellular carrier (pQYP) nor the carrier alone (TAT), reversed mechanical hypersensitivity caused by NGF (Fig. 2A). Pretreatment with TAT-pQYP or pan-PLC inhibitor, had the same impact over mechanical hypersensitivity, whereas control TAT-QYP had no effect (Fig. 2B).

The impact of inhibition of PLC<sub>γ</sub> (TAT-pQYP), PLCs (U-73122) (27), Trk (GNF-5837) (28), and TRPV1 (CPZ) (19) injected before CAP on CAP-elicited spontaneous nocifensive response was evaluated using the CAP test. Only the antagonism of TRPV1 by CPZ attenuated the assessed nociceptive phenotype (Fig. 2C). However, 2 h after CAP injection, TAT-pQYP and all inhibitors tested were able to prevent mechanical hypersensitivity (Fig. 2D), indicating the dependence of PLCγ, TrkA, and TRPV1 in this hypersensitivity mechanism.

## **Neurogenic Signaling in Nociceptors Promoted by CAP** Leads to Enhanced CGRP Signaling and Mast Cell Degranulation in a PLCγ-Independent Manner

Our data confirms a two-phase response elicited by CAP: an early chemonociceptive response and a later mechanical hypersensitive response as has been previously reported (29-31). Considering that TAT-pQYP had no effect on chemonociception, we next evaluated if it modulated neuropeptide signaling. We found that CGRP

was enhanced in ipsilateral DRG neurons after CAP injection, and this enhancement was not affected by prior injection of TAT-pQYP (Fig. 3, A and B).

Furthermore, glabrous skin of mice injected with CAP presented an increased mast cell recruitment and degranulation (Fig. 3, *C–F*), a phenomenon associated with SP signaling (32, 33), regardless of peptide pretreatment. Since Trk inhibitor demonstrated a similar effect to TAT-pQYP and PLC inhibition regarding mechanical sensitivity (Fig. 2D), we assessed Ngf mRNA expression after CAP injection in the paw soft tissues to confirm that this is an NGF-mediated mechanism. We observed that Ngf was enhanced in CAP-injected ipsilateral paws compared with the contralateral control (Fig. 3G). In addition, the mechanical hypersensitivity profile induced by CAP was similar to that induced by exogenous NGF injection (Fig. 3H), persisting for 24 h compared with the vehicle control. However, mechanical sensitivity did not return to baseline levels until 72 h consistent with the nociceptive pain average time course.

## PLCy Activity Promotes Mechanical Hypersensitivity Via NGF/TRPV1 in Nociceptors and Paw Diameter Increase Via VEGFA/eNOS in Endothelial Cells

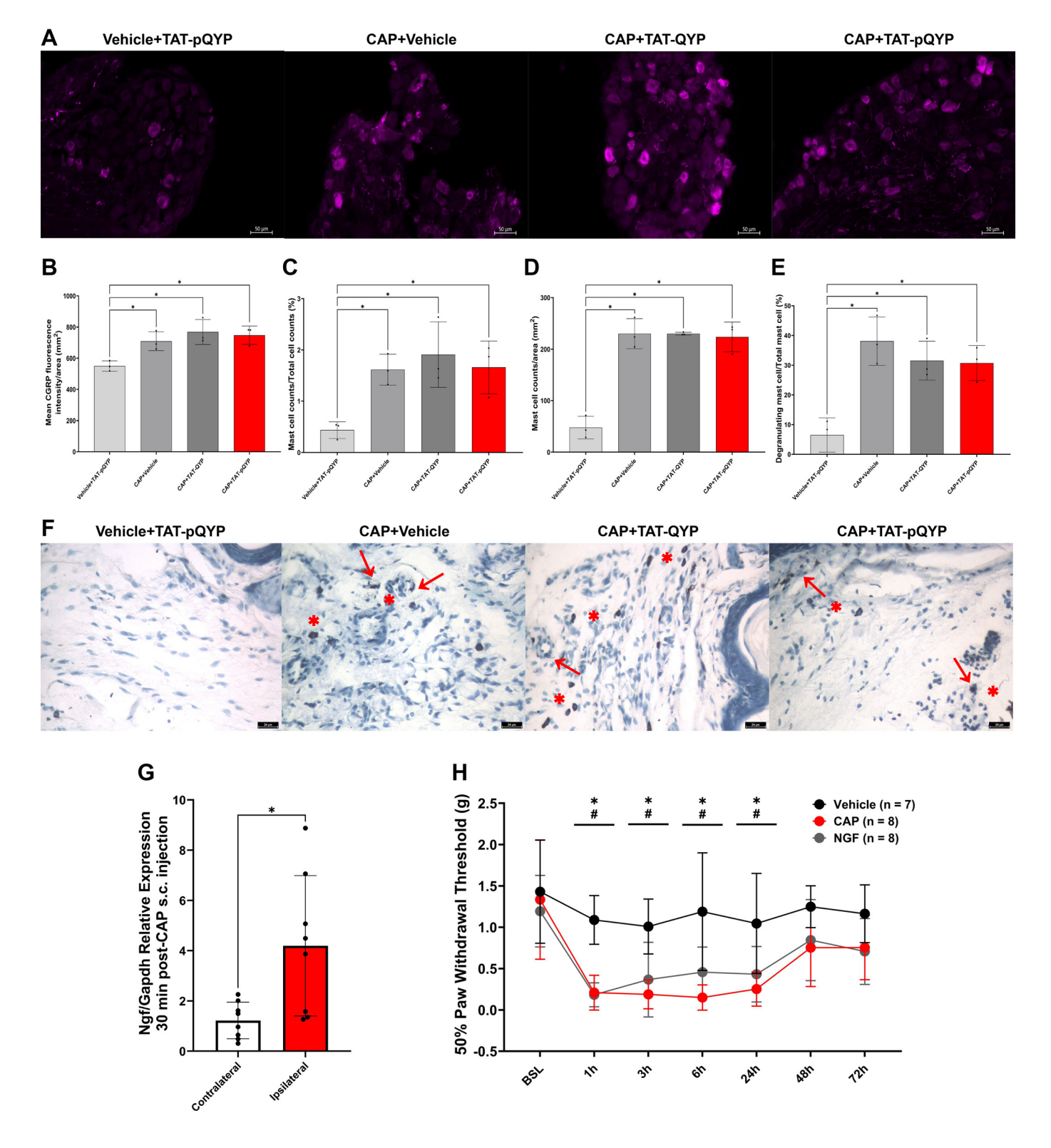
CAP-elicited mechanical hypersensitivity was further explored to assess the role of PLC<sub>\gamma</sub> up to 24 h postinjection, consistent with the hypersensitivity profile observed (Fig. 3H). TAT-pQYP, U-73122, GNF-5837, and CPZ, but not TAT-QYP, reverted the mechanical hypersensitivity threshold and had a sustained effect throughout 24 h post treatment (Fig. 4A). Given our previous finding that TATpQYP had a sustained effect for up to 6 h after treatment in the CFA model, upon which hypersensitivity was reestablished (17), we hypothesized that in the CAP model there was an additional effect of PLCγ aside from directly inhibiting PLC $\gamma$  in nociceptors to promote hypersensitivity.

To address this hypothesis, paw diameter was evaluated for up to 24 h to assess edema. We found that TAT-pQYP was able to attenuate paw diameter increase by 2 h after treatment compared with vehicle or TAT-QYP controls. TATpQYP was able to decrease paw diameter to a level comparable to vehicle injected mice at 4 h posttreatment (Fig. 4B). Regarding U-73122 and CPZ injection, paw diameter reached diameters of control animals only after 6 h posttreatment. On the other hand, GNF-5837 was not able to reach the diameter of control animals (Fig. 4B), indicating that TAT-pQYP could be affecting PLC<sub>\gamma</sub> activation through Trk-independent signaling pathways.

Vascular endothelial growth factor A (VEGFA) promotes vasodilation and plasma extravasation by interacting with its RTK (VEGFR2) in endothelial cells (34). We found

Figure 2. TAT-pQYP does not modulate nocifensive response related to TRPV1 direct sensitization by CAP, but reverses the mechanical hypersensitivity promoted by CAP. A: full length TAT-pQYP and U-73122 (PLC inhibitor), but not modified versions of the peptide (TAT, pQYP, and TAT-QYP), reverses mechanical hypersensitivity elicited by NGF subcutaneous injection (N = 7-8). B: TAT-pQYP, but not TAT-QYP, protects from mechanical hypersensitivity elicited by subcutaneous (sc) injection of NGF (N = 7-8). C. TAT-pQYP, U-73122, and GNF-5837 (pan-Trk inhibitor) did not alter the spontaneous nocifensive behavior elicited by CAP subcutaneous injection, which was only modulated by CPZ (TRPV1 inhibitor) (N = 8-9). D: TAT-pQYP, U-73122, GNF-5837, and CPZ rescued the mechanical threshold of CAP subcutaneous injected mice after 2 h (N = 6-9). N refers to number of animals used. Multiple comparison analysis was performed by two-way ANOVA in A, B, and D and one-way ANOVA in C, followed by Tukey's post hoc test to determine statistical significance. Results of each individual biological replicate are presented as black dots, and data are expressed and means ± SD. \*P < 0.05. BSL, baseline measure; CAP, capsaicin; CPZ, capsazepine; NGF, nerve growth factor; TRPV1, transient receptor potential cation channel, subfamily V, member 1. Experimental timeline images made with a licensed version of BioRender.com.

enhanced levels of Vegfa in soft tissues of paws injected with CAP compared with its contralateral control (Fig. 4C). Since, PLCγ can be phosphorylated/activated by VEGFR2, subsequently activating signaling cascades that culminates in phosphorylation of endothelial nitric oxide synthase (eNOS) at Ser<sup>1177</sup> via PKC, a key process for vasodilation/edema (35, 36), we evaluated phosphorylated eNOS protein levels in paws of injected mice 4 h after treatment, consistent with paw diameter normalization to control levels (Fig. 4B). TAT-pQYP led to a decrease in phosphorylated eNOS compared with TAT-QYP control (Fig. 4D).



To confirm that inflammation was in fact enhancing the nociceptive profile observed in CAP-injected mice during the timepoints where there is coexistence of mechanical hypersensitivity and increase in paw diameter (Fig. 4, A and B), we evaluated the mechanical sensitivity to innocuous and noxious touch, which are highly modulated by inflammatory responses (37), at the 4 h posttreatment point. As expected, we also found that TAT-pQYP was able to revert the associated hypersensitivity to innocuous touch and hypernociception to noxious stimuli as compared with TAT-QYP (Fig. 4, E and F).

## **DISCUSSION**

Neurogenic inflammation plays a significant role in many disease-mediated pain mechanisms. In migraine, CAP-sensitive peptidergic nociceptors have been implicated with plasma extravasation, vascular effects and hypersensitivity mechanisms linked to headache in a TRPV1-dependent manner (7, 38). Although enhanced SP, CGRP, and NGF levels are associated with pain intensity and frequency (39, 40). In psoriasis, TRPV1 and neuropeptides are upregulated and essential for driving skin inflammation (41-43), NGF is enhanced to promote itch and hypersensitivity (44) and involved with the increase in neuropeptides in DRG sensory neurons (45). Thus, both NGF and TRPV1-mediated signaling pathways are targets for treating these diseases.

Directly modulating TRPV1 promotes hyperthermia in mice and humans, followed by a subsequent desensitization and decreased expression of TRPV1, impairing heat sensitivity, essential for tissue preservation (14, 46). We previously proposed that disrupting protein-protein interactions (PPIs) in nociceptors may be a more effective strategy for developing analgesic treatments with fewer side effects compared with inhibiting the activity of channels and enzymes (47). In the present study, we propose that targeting the interaction between RTKs and PLC $\gamma$  in both nociceptors and endothelial cells is a strategy to attenuate the outcomes of neurogenic inflammation, including pain and edema, without disrupting TRPV1's physiological activity.

Considering that both chemonociception and neuropeptide release were unaffected by TAT-pQYP treatment, we propose that during CAP-triggered neurogenic inflammation, both the chemonociceptive phenotype and the proinflammatory peptidergic signaling are PLCγ-independent. CAP is capable of outcompeting the inhibitory PIP2 binding to TRPV1, activating the channel (10). Subsequent activation of mast cells leads to an inflammatory environment marked by NGF and VEGFA expression, initiating RTK- and PLCγdependent signaling pathways, modulated by TAT-pQYP in both nociceptors and endothelial cells, respectively. In nociceptors, TrkA phosphorylates PLCγ, releasing TRPV1 from PIP2 inhibition, activating PKC potentiation of channel activity, and promoting the observed hypersensitivity. In endothelial cells, VEGFR2 activates PLCγ, and in turn PKC, responsible for eNOS phosphorylation and the respective nitric oxide synthesis that promotes vasodilation (Fig. 5).

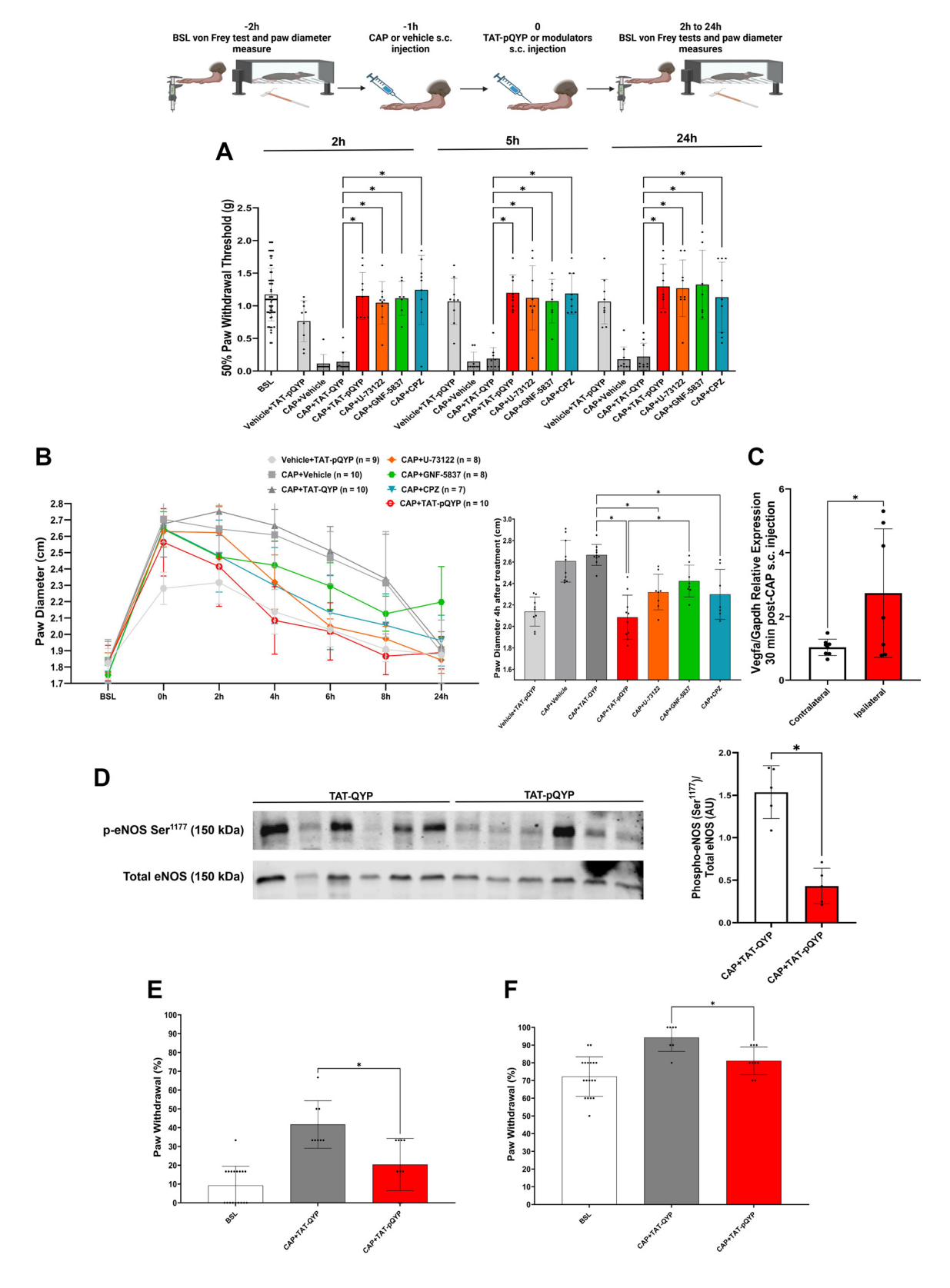
Furthermore, it is possible that the definitive effect of TAT-pQYP on nociception and inflammation is also supported by disruption in the positive neurogenic feedback mechanism that arises from NGF-TrkA signaling endosomes, which translocate to the DRG, amplifying PLCγ signaling (48, 49) further sensitizing TRPV1 (48), thus restarting the neurogenic loop. TAT-pQYP may also disrupt other PLCy-mediated effects, such as calcium/calmodulindependent kinase 2 (CaMKII) triggered by calcium signaling through IP3 receptors in the endoplasmic reticulum, leading to TRPV1 phosphorylation and activation of the transcription factor and cAMP-response element binding protein (CREB), responsible for an increase in expression of genes, determining nociceptor hyperactivity (50–53).

Here, we add evidence to the existing literature that blocking PLCγ or PLCs, in general, is an effective method to promote antinociception in both inflammatory and chronic pain models (17, 50-59). TAT-pQYP could be a lead compound for the development of small molecule analgesics selectively targeting PLC $\gamma$  with potentially fewer side effects than NGF/TrkA inhibitors. Though successful in mitigating pain, blocking NGF-NGFR signaling with NGF antibodies/ inhibitors impairs bone remodeling in osteoarthritic joints (60, 61). On the other hand, Trk inhibitors promote analgesia but can lead to paresthesia and withdrawal pain (62). Importantly, PLC signaling is key in several processes in the nervous system, as opposed to pan-PLC inhibitors, TATpQYP dampens PLCy signaling specifically, preserving other PLCs (17).

Recently, 2023, a mutation on Lys710 that interferes with TRPV1 activity led to the design of V1-cal peptide, that was able to prevent paw diameter increase and attenuate, but not suppress CGRP and SP enhanced expression in the DRG (63). TAT-pQYP did not modulate SP-related mast cells degranulation or CGRP enhanced expression in the DRG, which could explain why reestablishing the paw diameter to baseline levels is delayed.

Figure 3. TAT-pQYP does not modulate enhanced CGRP expression, nor act on mast cells recruitment or degranulation after CAP subcutaneous injection, which promotes the NGF-mediated mechanical hypersensitivity. A: representative sections of CGRP expressing DRG neurons with  $\times$ 200 magnification, which promotes the NGF-mediated mechanical hypersensitivity. tion from each experimental group (indicated above the sections). B: percentage of CGRP + cells in DRG neurons. Scale bar  $= 50 \,\mu m$ . C and D: mast cell infiltration to the hind paw's glabrous skin after CAP injection was determined relative to total cells (C) and image field area (D). E: CAP promotes mast cell degranulation, which is not modulated by TAT-pQYP treatment. F: representative sections of toluidine blue stained glabrous skin with a  $\times 400$ magnification from each experimental group (indicated above the sections). Red asterisks indicate regions of mast cells infiltration. Red arrows indicate mast cells degranulation. Scale bar = 24 µm. G: CAP subcutaneous injection induces enhanced Ngf mRNA expression in total extract of mice paws after 30 min (N = 8-9). H: CAP and NGF subcutaneous injection promotes similar mechanical hypersensitivity profiles that are statistically different to vehicle subcutaneous injected mice from 1 h to 24 h postinjection (N = 7 - 8). Two-way ANOVA, Tukey post hoc test. \*P < 0.05 to CAP vs. Vehicle; \*P < 0.05 to CAP vs. vehicle. Multiple comparison analysis was performed by one-way ANOVA in B-E (N=3), unpaired student's t test in G, and two-way ANOVA in H, followed by Tukey's post hoc test to determine significance, and data are expressed and means ± SD. N refers to number of animals or animal tissues used. \*P < 0.05. BSL, baseline measure; CAP, capsaicin; CGRP, calcitonin gene-related peptide; NGF, nerve growth factor.

A limitation of our study is that we only used male mice as a model, and although neurogenic inflammatory signaling in neurons may be similar between sexes in mice in naive conditions (64), the role of immune cells involved in the proposed mechanism may differ. Also, we cannot discard the possibility that TAT-pQYP acts through PLCγ-independent mechanisms by interfering with other SH2 domain containing proteins, however, similar effects were observed



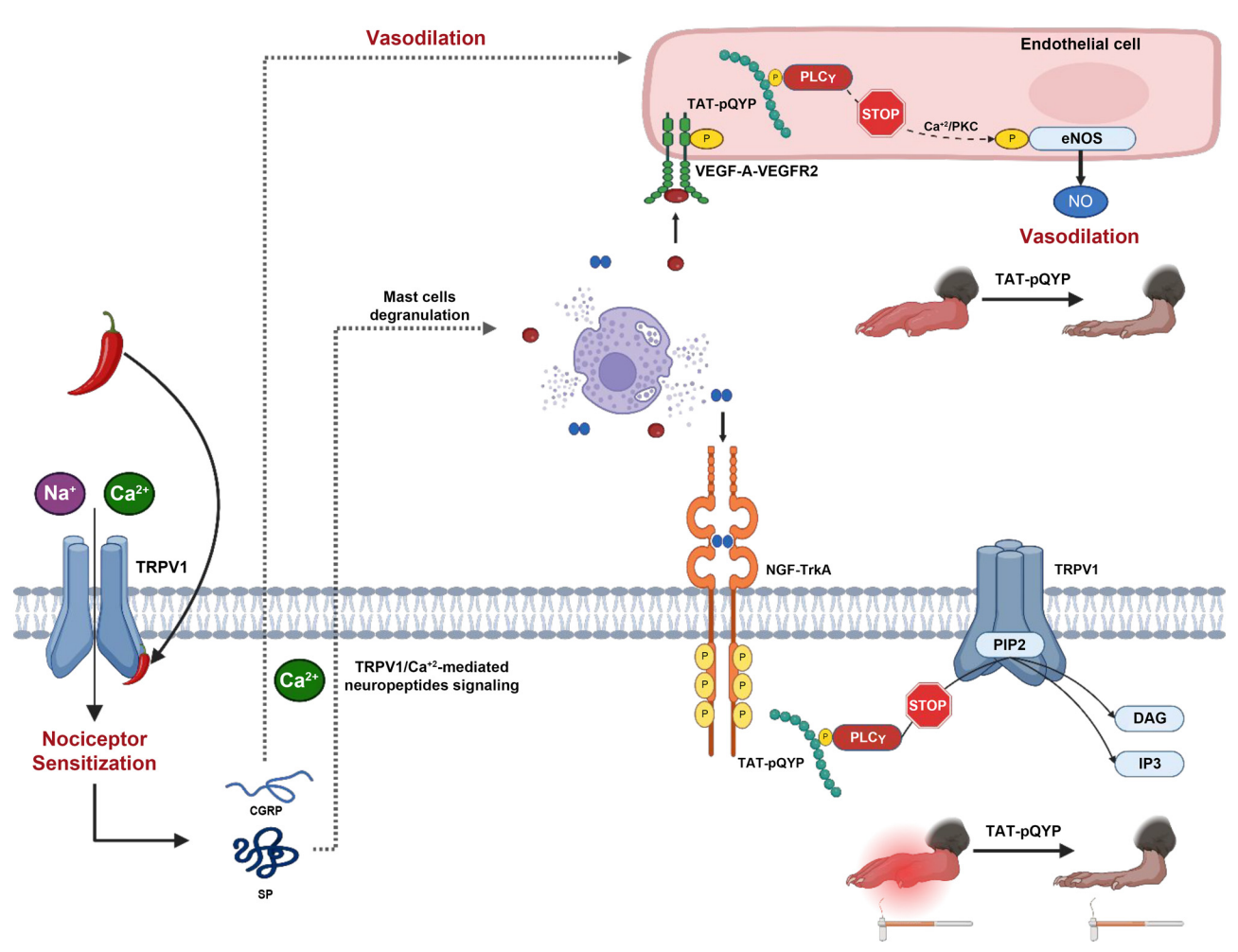


Figure 5. Proposed signaling pathways implicated in the dual effect of TAT-pQYP on nociception and endothelial cells induced by neurogenic stimuli. CAP directly opens TRPV1 in nociceptors to induce spontaneous burning and itching related chemonociceptive behavior. Cations enter through TRPV1, enhancing proinflammatory neuropeptides CGRP and SP signaling in peptidergic nociceptors, initiating neurogenic inflammation. CGRP can act directly on endothelial cells to promote vasodilation and SP activation of mast cells leads to degranulation and release of inflammatory factors, such as growth factors NGF and VEGFA. The latter promote autophosphorylation/activation of their respective RTKs, TrkA (nociceptors), and VEGFR2 (endothelial cells) and activation of downstream signaling (PLC\(\gamma/PKC\)). TAT-pQYP inhibits the interaction between PLC\(\gamma\) and RTKs, preventing eNOS phosphorylation in endothelial cells, which inhibits vasodilation through nitric oxide (NO) signaling, and favoring the closed state of TRPV1 by sustained PIP2 in nociceptors, preventing hypersensitivity and the neuro-immune inflammatory loop. CAP, capsaicin; pholipase C-γ, RTKs, receptor tyrosine kinase; SP, substance P; TrkA, tropomyosin kinase A; TRPV1, transient receptor potential cation channel, subfamily V, member 1. Figure created with a licensed version of BioRender.com.

using a pan-PLC inhibitor, suggesting that PLC $\gamma$  is a main component in neurogenic inflammation and a good pharmacological target for the development of non-opioid analgesics for inflammatory pain. Finally, we pave the way for future studies to address the role of RTKs, and specifically for PLCγ, in other pain models and suggest the lipase as a promising target for diseases mediated by neurogenic inflammation.

Figure 4. TAT-pQYP treatment after CAP subcutaneous injection rescues mechanical threshold and modulates paw diameter increase acting on endothelial cells. A: TAT-pQYP, as U-73122 (PLC inhibitor), GNF-5837 (Trk inhibitor), and CPZ (TRPV1 inhibitor), rescued the mechanical threshold when injected after CAP (N = 9). B: TAT-pQYP, U-73122, and CPZ reverses paw diameter increase after CAP subcutaneous injection (left). Highlight on the 4 h time point of paw diameter measures (right) (N = 7-10). C: CAP subcutaneous injection enhances Vegfa mRNA expression in total extract of mice paws after 30 min (N = 7). D: TAT-pQYP inhibited phosphorylation of eNOS Ser1177 compared with TAT-QYP 4 h after treatment (N = 5; 1 outlier excluded for each group - lanes 4 and 10). E: TAT-pQYP, but not TAT-QYP, rescues paw withdrawal percentages for innocuous mechanical stimuli (0.07 g von Frey) (N = 9–10). F: TAT-pQYP, but not TAT-QYP, rescues paw withdrawal percentages for noxious mechanical stimuli (24 G needle pin-prick) (N = 9–10). Each individual biological replicate results are presented as black dots in graphs. N refers to number of animals or animal tissues used. Multiple comparison analysis was performed by two-way ANOVA in A, B, E, and F and unpaired student's t test in C and D, followed by Tukey's post hoc test to determine statistical significance. Experimental timelines of each approach are presented above the respective results sets. Data are expressed and means  $\pm$  SD. \*P < 0.05. BSL, baseline measure; CAP, capsaicin; CPZ, capsazepine; TRPV1, transient receptor potential cation channel, subfamily V, member 1; VEGFA, vascular endothelial growth factor A. Experimental timeline images made with a licensed version of BioRender.com.



## DATA AVAILABILITY

The data that support the findings of this study are available in the MATERIALS AND METHODS and RESULTS of the manuscript. Raw data are available from the corresponding authors upon request.

# **ACKNOWLEDGMENTS**

Dr. Heloisa A. Mattielo for general technical assistance in tissue extraction. Dr. Felipe M. Vieceli for technical aid with microscopy.

#### **GRANTS**

This work was supported by FAPESP (Fundação de Amparo à Pesquisa do Estado de São Paulo): Grant No. 2019/06982-6 (to D.S. and C.S.D.), fellowship No. 2022/00594-7 (to B.C.d.M.), fellowship No. 24/20449-7 (to R.S.S.), fellowship No. 2023/10572-3 (to A.M.R.), fellowship No. 2023/09168-3 (to H.E.G.R.); CNPg (Conselho Nacional de Desenvolvimento Científico e Tecnológico): fellowship PQ-2 No. 307739/2018-0 (to D.S.); CAPES (Coordenação de Aperfeiçoamento de Pessoal de Nível Superior) fellowship No. 88887.825233/2023-00 (to A.M.d.N.).

## **DISCLOSURES**

No conflicts of interest, financial or otherwise, are declared by the authors.

## **AUTHOR CONTRIBUTIONS**

A.M.d.N. and D.S. conceived and designed research; A.M.d.N., A.M.R., H.E.G.R., B.C.d.M., and R.S.S. performed experiments; A.M.d.N. analyzed data; A.M.d.N. and D.S. interpreted results of experiments; A.M.d.N. prepared figures; A.M.d.N. and D.S. drafted manuscript; A.M.d.N. and D.S. edited and revised manuscript; A.M.d.N., A.M.R., B.C.d.M., H.E.G.R., R.S.S., C.S.D., and D.S. approved final version of manuscript.

#### **REFERENCES**

- Raja SN, Carr DB, Cohen M, Finnerup NB, Flor H, Gibson S, Keefe FJ, Mogil JS, Ringkamp M, Sluka KA, Song X-J, Stevens B, Sullivan MD, Tutelman PR, Ushida T, Vader K. The revised International Association for the Study of Pain definition of pain: concepts, challenges, and compromises. Pain 161: 1976–1982, 2020. doi:10.1097/j. pain.000000000001939.
- Caterina MJ, Schumacher MA, Tominaga M, Rosen TA, Levine JD, Julius D. The capsaicin receptor: a heat-activated ion channel in the pain pathway. Nature 389: 816-824, 1997. doi:10.1038/39807.
- Kwon DH, Zhang F, Suo Y, Bouvette J, Borgnia MJ, Lee S-Y. Heatdependent opening of TRPV1 in the presence of capsaicin. Nat Struct Mol Biol 28: 554-563, 2021. doi:10.1038/s41594-021-00616-3.
- Caterina MJ, Julius D. The vanilloid receptor: a molecular gateway to the pain pathway. Annu Rev Neurosci 24: 487-517, 2001. doi:10. 1146/annurev.neuro.24.1.487.
- Leon A, Buriani A, Dal Toso R, Fabris M, Romanello S, Aloe L, Levi-Montalcini R. Mast cells synthesize, store, and release nerve growth factor. Proc Natl Acad Sci USA 91: 3739-3743, 1994. doi:10.1073/ pnas.91.9.3739.
- Gupta K, Harvima IT. Mast cell-neural interactions contribute to pain and itch. Immunol Rev 282: 168-187, 2018. doi:10.1111/imr.12622.
- Dux M, Sántha P, Jancsó G. Capsaicin-sensitive neurogenic sensory vasodilatation in the dura mater of the rat. J Physiol 552: 859-867, 2003. doi:10.1113/jphysiol.2003.050633.
- Chuang H, Prescott ED, Kong H, Shields S, Jordt S-E, Basbaum AI, Chao MV, Julius D. Bradykinin and nerve growth factor release the capsaicin receptor from PtdIns(4,5)P2-mediated inhibition. Nature 411: 957-962, 2001. doi:10.1038/35082088.
- McKelvey L, Shorten GD, O'Keeffe GW. Nerve growth factor-mediated regulation of pain signalling and proposed new intervention

- strategies in clinical pain management. J Neurochem 124: 276-289, 2013. doi:10.1111/jnc.12093.
- Arnold WR, Mancino A, Moss FR, Frost A, Julius D, Cheng Y. Structural basis of TRPV1 modulation by endogenous bioactive lipids. Nat Struct Mol Biol 31: 1377-1385, 2024. doi:10.1038/s41594-024-01299-2.
- Joseph J, Qu L, Wang S, Kim M, Bennett D, Ro J, Caterina MJ, Chung M-K. Phosphorylation of TRPV1 S801 contributes to modalityspecific hyperalgesia in mice. J Neurosci 39: 9954–9966, 2019. doi:10.1523/JNEUROSCI.1064-19.2019.
- Obeidat AM, Donner A, Miller RE. An update on targets for treating osteoarthritis pain: NGF and TRPV1. Curr Treatm Opt Rheumatol 6: 129-145, 2020. doi:10.1007/s40674-020-00146-x.
- Schmelz M, Mantyh P, Malfait A-M, Farrar J, Yaksh T, Tive L, Viktrup L. Nerve growth factor antibody for the treatment of osteoarthritis pain and chronic low-back pain: mechanism of action in the context of efficacy and safety. Pain 160: 2210-2220, 2019. doi:10. 1097/j.pain.0000000000001625.
- Garami A, Shimansky YP, Rumbus Z, Vizin RCL, Farkas N, Hegyi J, Szakacs Z, Solymar M, Csenkey A, Chiche DA, Kapil R, Kyle DJ, Van Horn WD, Hegyi P, Romanovsky AA. Hyperthermia induced by transient receptor potential vanilloid-1 (TRPV1) antagonists in human clinical trials: Insights from mathematical modeling and meta-analysis. Pharmacol Ther 208: 107474, 2020. doi:10.1016/j.pharmthera. 2020.107474.
- 15 Hunter P. New therapies to relieve pain. EMBO Rep 19: e46925, 2018. doi:10.15252/embr.201846925.
- Wieczorek S, Bergström J, Sääf M, Kötting J, Iwarsson E. 16. Expanded HSAN4 phenotype associated with two novel mutations in NTRK1. Neuromuscul Disord 18: 681–684, 2008. doi:10.1016/j.nmd. 2008.06.370.
- Moraes BC, Ribeiro-Filho HV, Roldão AP, Toniolo EF, Carretero GPB, Sgro GG, Batista FAH, Berardi DE, Oliveira VRS, Tomasin R, Vieceli FM, Pramio DT, Cardoso AB, Figueira ACM, Farah SC, Devi LA, Dale CS, de Oliveira PSL, Schechtman D. Structural analysis of TrkA mutations in patients with congenital insensitivity to pain reveals PLCγ as an analgesic drug target. Sci Signal 15: eabm6046, 2022. doi:10.1126/scisignal.abm6046.
- Percie Du Sert N, Ahluwalia A, Alam S, Avey MT, Baker M, Browne WJ, Clark A, Cuthill IC, Dirnagl U, Emerson M, Garner P, Holgate ST, Howells DW, Hurst V, Karp NA, Lazic SE, Lidster K, MacCallum CJ, Macleod M, Pearl EJ, Petersen OH, Rawle F, Reynolds P, Rooney K, Sena ES, Silberberg SD, Steckler T, Würbel H. Reporting animal research: explanation and elaboration for the ARRIVE guidelines 2.0. PLoS Biol 18: e3000411, 2020. doi:10.1371/journal.pbio. 3000411.
- Sakurada T, Matsumura T, Moriyama T, Sakurada C, Ueno S, Sakurada S. Differential effects of intraplantar capsazepine and ruthenium red on capsaicin-induced desensitization in mice. Pharmacol Biochem Behav 75: 115-121, 2003. doi:10.1016/S0091-3057(03)00066-2.
- Khodorova A, Nicol GD, Strichartz G. The p75NTR signaling cascade mediates mechanical hyperalgesia induced by nerve growth factor injected into the rat hind paw. Neuroscience 254: 312-323, 2013. doi:10.1016/j.neuroscience.2013.09.046.
- Vyas PM, Payne RM. TAT opens the door. Mol Ther 16: 647-648, 2008. doi:10.1038/mt.2008.24
- Chaplan SR, Bach FW, Pogrel JW, Chung JM, Yaksh TL. Quantitative assessment of tactile allodynia in the rat paw. J Neurosci Methods 53: 55-63, 1994. doi:10.1016/0165-0270(94)90144-9.
- Duan B, Cheng L, Bourane S, Britz O, Padilla C, Garcia-Campmany L, Krashes M, Knowlton W, Velasguez T, Ren X, Ross SE, Lowell BB, Wang Y, Goulding M, Ma Q. Identification of spinal circuits transmitting and gating mechanical pain. Cell 159: 1417-1432, 2014. doi:10.1016/j.cell.2014.11.003.
- Kozera B, Rapacz M. Reference genes in real-time PCR. J Appl Genet 54: 391-406, 2013. doi:10.1007/s13353-013-0173-x.
- Meloto CB, Ingelmo P, Perez EV, Pitt R, González Cárdenas VH, Mohamed N, Sotocinal SG, Bourassa V, Lima LV, Ribeiroda-Silva A, Mogil JS, Diatchenko L. Mast cell stabilizer ketotifen fumarate reverses inflammatory but not neuropathic-induced mechanical pain in mice. Pain Rep 6: e902, 2021. doi:10.1097/ PR9.0000000000000902.

- 26. Heemskerk FMJ, Chen HC, Huang FL. Protein kinase C phosphorylates Ser152, Ser156 and Ser163 but not Ser160 of MARCKS in rat brain. Biochem Biophys Res Commun 190: 236-241, 1993. doi:10. 1006/bbrc.1993.1036.
- 27. Hou C, Kirchner T, Singer M, Matheis M, Argentieri D, Cavender D. In vivo activity of a phospholipase C inhibitor, 1-(6-((17β -3-methoxyestra-1,3,5(10)-trien-17-yl)amino)hexyl)-1H-pyrrole-2,5-dione (U73122), in acute and chronic inflammatory reactions. J Pharmacol Exp Ther 309: 697-704, 2004. doi:10.1124/jpet.103.060574.
- Shutov LP, Warwick CA, Shi X, Gnanasekaran A, Shepherd AJ, Mohapatra DP, Woodruff TM, Clark JD, Usachev YM. The complement system component C5a produces thermal hyperalgesia via macrophage-to-nociceptor signaling that requires NGF and TRPV1. J Neurosci 36: 5055-5070, 2016. doi:10.1523/JNEUROSCI.3249-15.
- Entrena JM, Cobos EJ, Nieto FR, Cendán CM, Baeyens JM, Del Pozo E. Antagonism by haloperidol and its metabolites of mechanical hypersensitivity induced by intraplantar capsaicin in mice: role of sigma-1 receptors. Psychopharmacology (Berl) 205: 21-33, 2009. doi:10.1007/s00213-009-1513-8.
- 30. Entrena JM, Sánchez-Fernández C, Nieto FR, González-Cano R, Yeste S, Cobos EJ, Baeyens JM. Sigma-1 receptor agonism promotes mechanical allodynia after priming the nociceptive system with capsaicin. Sci Rep 6: 37835, 2016. doi:10.1038/srep37835.
- Joshi SK, Hernandez G, Mikusa JP, Zhu CZ, Zhong C, Salyers A, Wismer CT, Chandran P, Decker MW, Honore P. Comparison of antinociceptive actions of standard analgesics in attenuating capsaicin and nerve-injury-induced mechanical hypersensitivity. Neuroscience 143: 587-596, 2006. doi:10.1016/j.neuroscience. 2006.08.005.
- 32. Suzuki H, Miura S, Liu YY, Tsuchiya M, Ishii H. Substance P induces degranulation of mast cells and leukocyte adhesion to venular endothelium. Peptides 16: 1447-1452, 1995. doi:10.1016/ 0196-9781(95)02050-0.
- Mousavizadeh R, Waugh CM, McCormack RG, Cairns BE, Scott A. MRGPRX2-mediated mast cell activation by substance P from overloaded human tenocytes induces inflammatory and degenerative responses in tendons. Sci Rep 14: 13540, 2024. doi:10.1038/s41598-024-64222-1.
- **Chen D**, **Simons M**. Emerging roles of PLC $\gamma$ 1 in endothelial biology. Sci Signal 14: eabc6612, 2021. doi:10.1126/scisignal.abc6612.
- Partovian C, Zhuang Z, Moodie K, Lin M, Ouchi N, Sessa WC, Walsh K. Simons M. PKCα activates eNOS and increases arterial blood flow in vivo. Circ Res 97: 482-487, 2005. doi:10.1161/01.RES. 0000179775.04114.45.
- Dudzinski D, Michel T. Life history of eNOS: partners and pathways. Cardiovasc Res 75: 247-260, 2007. doi:10.1016/j.cardiores.2007.03.
- Coutaux A, Adam F, Willer JC, Le Bars D. Hyperalgesia allodynia: peripheral mechanisms. J Bone Joint Spine 72: 359-371, 2005. doi:10.1016/J.JBSPIN.2004.01.010.
- Markowitz S, Saito K, Moskowitz M. Neurogenically mediated leakage of plasma protein occurs from blood vessels in dura mater but not brain. J Neurosci 7: 4129-4136, 1987. doi:10.1523/JNEUROSCI. 07-12-04129.1987.
- Jang M, Park J, Kho H, Chung S, Chung J. Plasma and saliva levels of nerve growth factor and neuropeptides in chronic migraine patients. Oral Dis 17: 187-193, 2011. doi:10.1111/j.1601-0825.2010.
- Mozafarihashjin M, Togha M, Ghorbani Z, Farbod A, Rafiee P, Martami F. Assessment of peripheral biomarkers potentially involved in episodic and chronic migraine: a case-control study with a focus on NGF, BDNF, VEGF, and PGE2. J Headache Pain 23: 3, 2022. doi:10.1186/s10194-021-01377-6.
- Riol-Blanco L, Ordovas-Montanes J, Perro M, Naval E, Thiriot A, Alvarez D, Paust S, Wood JN, von Andrian UH. Nociceptive sensory neurons drive interleukin-23-mediated psoriasiform skin inflammation. Nature 510: 157-161, 2014. doi:10.1038/nature13199.
- Guo J, Qi C, Liu Y, Guo X, Meng Y, Zhao J, Fu J, Di T, Zhang L, Guo X, Liu Q, Wang Y, Li P, Wang Y. Terrestrosin D ameliorates skin lesions in an imiquimod-induced psoriasis-like murine model by inhibiting the interaction between Substance P and Dendritic cells. Phytomedicine 95: 153864, 2022. doi:10.1016/j.phymed. 2021.153864.

- Dainichi T, Kitoh A, Otsuka A, Nakajima S, Nomura T, Kaplan DH, Kabashima K. The epithelial immune microenvironment (EIME) in atopic dermatitis and psoriasis. Nat Immunol 19: 1286–1298, 2018. doi:10.1038/s41590-018-0256-2.
- Nakamura M, Toyoda M, Morohashi M. Pruritogenic mediators in psoriasis vulgaris: comparative evaluation of itch-associated cutaneous factors. Br J Dermatol 149: 718-730, 2003. doi:10.1046/j.1365-2133.2003.05586.x.
- Joachim RA, Kuhlmei A, Dinh QT, Handjiski B, Fischer T, Peters EMJ, Klapp BF, Paus R, Arck PC. Neuronal plasticity of the "brainskin connection": stress-triggered up-regulation of neuropeptides in dorsal root ganglia and skin via nerve growth factor-dependent pathways. J Mol Med (Berl) 85: 1369-1378, 2007. doi:10.1007/ s00109-007-0236-8.
- Rosenberger DC, Binzen U, Treede R-D, Greffrath W. The capsaicin receptor TRPV1 is the first line defense protecting from acute non damaging heat: a translational approach. J Transl Med 18: 28, 2020. doi:10.1186/s12967-019-02200-2.
- do Nascimento AM, Marques RB, Roldão AP, Rodrigues AM, Eslava RM, Dale CS, Reis EM, Schechtman D. Exploring proteinprotein interactions for the development of new analgesics. Sci Signal 17: eadn4694, 2024. doi:10.1126/scisignal.adn4694.
- Zhu W, Oxford GS. Phosphoinositide-3-kinase and mitogen activated protein kinase signaling pathways mediate acute NGF sensitization of TRPV1. Mol Cell Neurosci 34: 689-700, 2007. doi:10.1016/j. mcn.2007.01.005.
- Marlin MC, Li G. Biogenesis and function of the NGF/TrkA signaling endosome. Int Rev Cell Mol Biol 314: 239-257, 2015. doi:10.1016/bs. ircmb.2014.10.002.
- Masuoka T, Yamashita Y, Yoshida J, Nakano K, Tawa M, Nishio M, Ishibashi T. Sensitization of glutamate receptor-mediated pain behaviour via nerve growth factor-dependent phosphorylation of transient receptor potential V1 under inflammatory conditions. Br J Pharmacol 177: 4223-4241, 2020. doi:10.1111/bph.15176.
- Xia C, Shen S, Hashmi F, Qiao LY. Colitis-induced bladder afferent neuronal activation is regulated by BDNF through PLCγ pathway. Exp Neurol 285: 126-135, 2016. doi:10.1016/j.expneurol.2015.12.006.
- Hashmi F, Liu M, Shen S, Qiao L-Y. Phospholipase C gamma mediates endogenous brain-derived neurotrophic factor-requlated calcitonin gene-related peptide expression in colitisinduced visceral pain. Mol Pain 12: 1744806916657088, 2016. doi:10.1177/1744806916657088.
- Xie A, Zhang X, Ju F, Zhou Y, Wu D, Han J. Sevoflurane impedes neuropathic pain by maintaining endoplasmicreticulum stress and oxidative stress homeostasis through inhibiting the activation of the PLCγ/CaMKII/IP3R signaling pathway. Aging (Albany NY) 16: 11062-11071, 2024. doi:10.18632/aging.206001.
- Shi T-JS, Liu S-XL, Hammarberg H, Watanabe M, Xu Z-QD, Hökfelt T. Phospholipase  $C\beta 3$  in mouse and human dorsal root ganglia and spinal cord is a possible target for treatment of neuropathic pain. Proc Natl Acad Sci USA 105: 20004-20008, 2008. doi:10.1073/ pnas.0810899105.
- Zhou JZ, Chen H, Xu WL, Fu Z, Zhou S, Zhu WJ, Zhang ZH. Auricular vagal nerve stimulation inhibited central nerve growth factor/tropomyosin receptor kinase A/phospholipase C-gamma signaling pathway in functional dyspepsia model rats with gastric hypersensitivity. Neuromodulation 27: 273–283, 2024. doi:10.1016/j. neurom.2023.01.007.
- Joseph EK, Bogen O, Alessandri-Haber N, Levine JD. PLC-β3 signals upstream of PKCε in acute and chronic inflammatory hyperalgesia. Pain 132: 67-73, 2007. doi:10.1016/j.pain.2007.01.027.
- Chen Y, Yang C, Wang ZJ. Proteinase-activated receptor 2 sensitizes transient receptor potential vanilloid 1, transient receptor potential vanilloid 4, and transient receptor potential ankyrin 1 in paclitaxel-induced neuropathic pain. Neuroscience 193: 440-451, 2011. doi:10.1016/j.neuroscience.2011.06.085.
- Wang S, Dai Y, Fukuoka T, Yamanaka H, Kobayashi K, Obata K, Cui X, Tominaga M, Noguchi K. Phospholipase C and protein kinase A mediate bradykinin sensitization of TRPA1: a molecular mechanism of inflammatory pain. Brain 131: 1241–1251, 2008. doi:10. 1093/brain/awn060.
- Tang H-B, Inoue A, Oshita K, Nakata Y. Sensitization of vanilloid receptor 1 induced by bradykinin via the activation of second

- messenger signaling cascades in rat primary afferent neurons.  $Eur\,J$ Pharmacol 498: 37-43, 2004. doi:10.1016/j.ejphar.2004.07.076.
- Hochberg MC, Carrino JA, Schnitzer TJ, Guermazi A, Walsh DA, White A, Nakajo S, Fountaine RJ, Hickman A, Pixton G, Viktrup L, Brown MT, West CR, Verburg KM. Long-term safety and efficacy of subcutaneous tanezumab versus nonsteroidal antiinflammatory drugs for hip or knee osteoarthritis: a randomized trial. Arthritis Rheumatol 73: 1167-1177, 2021. doi:10.1002/art.41674.
- Zhao L, Lai Y, Jiao H, Huang J. Nerve growth factor receptor limits inflammation to promote remodeling and repair of osteoarthritic joints. Nat Commun 15: 3225, 2024. doi:10.1038/s41467-024-47633-6.
- 62. Liu D, Flory J, Lin A, Offin M, Falcon CJ, Murciano-Goroff YR, Rosen E, Guo R, Basu E, Li BT, Harding JJ, Iyer G, Jhaveri K,
- Gounder MM, Shukla NN, Roberts SS, Glade-Bender J, Kaplanis L, Schram A, Hyman DM, Drilon A. Characterization of on-target adverse events caused by TRK inhibitor therapy. Ann Oncol 31: 1207-1215, 2020. doi:10.1016/j.annonc.2020.05.006.
- He S, Zambelli VO, Sinharoy P, Brabenec L, Bian Y, Rwere F, Hell RCR, Stein Neto B, Hung B, Yu X, Zhao M, Luo Z, Wu C, Xu L, Svensson KJ, McAllister SL, Stary CM, Wagner N-M, Zhang Y, Gross ER. A human TRPV1 genetic variant within the channel gating domain regulates pain sensitivity in rodents. J Clin Invest 133: e163735, 2023. doi:10.1172/JCI163735.
- Zheng Y, Liu P, Bai L, Trimmer JS, Bean BP, Ginty DD. Deep sequencing of somatosensory neurons reveals molecular determinants of intrinsic physiological properties. Neuron 103: 598-616.e7, 2019. doi:10.1016/j.neuron.2019.05.039.